Human Molecular Genetics, 2012, Vol. 21, No. 8 **1760–1769**
doi:10.1093/hmg/ddr609
Advance Access published on January 3, 2012

parkin-induced defects in neurophysiology and locomotion are generated by metabolic dysfunction and not oxidative stress

Amanda Vincent, Laura Briggs, Griff F.J. Chatwin, Elizabeth Emery, Rose Tomlins, Matt Oswald†, C. Adam Middleton, Gareth J.O. Evans, Sean T. Sweeney and Christopher J.H. Elliott*

Department of Biology, University of York, PO Box 373, York YO10 5YW, UK

Received October 26, 2011; Revised and Accepted December 21, 2011

Parkinson's disease (PD) is characterized by movement disorders, including bradykinesia. Analysis of inherited, juvenile PD, identified several genes linked via a common pathway to mitochondrial dysfunction. In this study, we demonstrate that the larva of the *Drosophila parkin* mutant faithfully models the locomotory and metabolic defects of PD and is an excellent system for investigating their inter-relationship. *parkin* larvae displayed a marked bradykinesia that was caused by a reduction in both the frequency of peristalsis and speed of muscle contractions. Rescue experiments confirmed that this phenotype was due to a defect in the nervous system and not in the muscle. Furthermore, recordings of motoneuron activity in *parkin* larvae revealed reduced bursting and a striking reduction in evoked and miniature excitatory junction potentials, suggesting a neuronal deficit. This was supported by our observations in *parkin* larvae that the resting potential was depolarized, oxygen consumption and ATP concentration were drastically reduced while lactate was increased. These findings suggest that neuronal mitochondrial respiration is severely compromised and there is a compensatory switch to glycolysis for energy production.

***parkin* mutants also possessed overgrown neuromuscular synapses, indicative of oxidative stress, which could be rescued by overexpression of *parkin* or scavengers of reactive oxygen species (ROS). Surprisingly, scavengers of ROS did not rescue the resting membrane potential and locomotory phenotypes. We therefore propose that mitochondrial dysfunction in *parkin* mutants induces Parkinsonian bradykinesia via a neuronal energy deficit and resulting synaptic failure, rather than as a consequence of downstream oxidative stress.**

INTRODUCTION

The recognition of Mendelian inheritance in some forms of Parkinson's disease (PD) has revolutionized our understanding of the causation of this disease (1). Mutations in PD-related genes (e.g. *parkin*, *α-synuclein*, *PINK1*, *LRRK2*) have now been replicated in a range of model organisms (2). *Drosophila* models share many features with the human disease, including the loss of dopaminergic neurons in the central nervous system (CNS) and reduced locomotion. Other similarities are evident at the cellular level, particularly mitochondrial malfunction and disorganization (3–5). The advanced fly genetic toolbox (6) has also facilitated deep insights into the cellular and metabolic pathways in which the PD-related gene products participate. A key result has been the identification of a single cellular pathway focussing on 4E-BP, to which several genes (*parkin*, *PINK1* and *LRRK2*) contribute (7), suggesting the potential for novel drug therapies across several genotypes.

Apart from dopaminergic cell death, few *Drosophila* studies have analysed neuronal phenotypes, focusing instead on spermatozoa, eye or muscle. Our first focus, therefore, is what are the neurophysiological (rather than muscle) defects that lead to reduced locomotion? For this, we turned our attention to the larval (juvenile) system, as it helps us understand

*To whom correspondence should be addressed. Tel: +44 1904328654; Fax: +44 1904328505; Email: cje2@york.ac.uk
†Present address: Department of Zoology, University of Cambridge, Downing Street, Cambridge CB2 3EJ, UK.

the initial stages of the neurodegenerative process. The larval neuromuscular junction is one of the best-characterized synapses (8). It is essential for normal movement. Here, we describe our finding that *parkin* mutant larvae have defective locomotion, with a bradykinesia-like phenotype. This is accompanied by reduced resting and synaptic potentials. The inability to maintain the normal muscle resting potential suggested that the mitochondria could not produce enough ATP: indeed, we find that *parkin* larvae have reduced ATP and oxygen consumption. Furthermore, they have elevated lactate, indicating that glycolysis may be elevated in response to the ATP deficit.

Our second question is how does oxidative stress relate to mitochondrial dysfunction? Fly models of PD are highly sensitive to oxidative stress, for example to paraquat (9,10), and are rescued by overexpression of genes that reduce reactive oxygen species (ROS) (11–14). It has recently been recognized that oxidative stress induces autophagy and synaptic overgrowth (15,16). We find that *parkin* mutants indeed have synaptic overgrowth, and this is rescued by overexpression of ROS scavengers as well as by *parkin.* However, as we find that ROS scavengers do not rescue the locomotion or electrophysiological defects, we are genetically separating the fundamental *parkin* deficit of energy production from its downstream oxidative stress consequences.

RESULTS

parkin larvae move slowly

The tracks of *parkin* mutant larvae crawling across an agar plate are shorter for animals migrating for a set interval of time (2 min) than wild-type as the *parkin* larvae move more slowly (Fig. 1A). Their mean speed is reduced to 62% of the wild-type. The *parkin* heterozygote crawls at the same speed as the wild-type, as would be expected from this recessive mutation. Using the GAL4/UAS system, we tested for rescue by global expression of wild-type *parkin* in the mutant background and found the velocity to be fully restored. As *parkin* mutants have both neuronal (11) and muscle (17) phenotypes, we then tested for tissue-specific rescue using neuronal (using *elav* GAL4) and muscle (*G14* GAL4) drivers. The neuronal driver rescued locomotion to wild-type levels, but no significant rescue was achieved with the muscle driver (Fig. 1B). We confirmed the data from Figure 1 using two additional wild-types, a second heterozygote and two other *parkin* mutant combinations, with both the $park^{25}$ homozygote null and $park^{z3678}$ hypomorph crawling more slowly than the other genotypes (*CS*, w^-, $CS/park^{25}$, nested ANOVA, *parkin* versus wild-types; $F_{1,113} = 34$, $P < 0.001$). Further confirmation of the role of neuronal parkin in locomotion was provided by using the same drivers to test for rescue in the $park^{25}$ homozygote background. The global (*Act5C* GAL4) or neuronal drivers gave partial rescue (71% and 77%, respectively, nested ANOVA $F_{77,1} = 7.4$, $P = 0.008$) but no rescue was seen using the muscle driver (mean larval speed 93% of the $park^{25}$ homozygote, ANOVA, Bonferroni *post hoc* test, $P = 1.0$).

We assayed the strength and frequency of peristaltic contractions directly, using a larval length assay, in which a restrained larva pulls on a flexible beam (Fig. 2A). Wild-type larvae pulled regularly on the beam, while the *parkin* knockouts had a reduced frequency of contractions (32% of wild-type; Fig. 2B and D). However, the peak–peak change in length did not differ between the wild-type and *parkin* null (Fig. 2C). This suggests that the reduced velocity of the larvae was due to less frequent steps, rather than a reduced step size. A particular feature of the *parkin* larval contractions was the slow rate at which the larva shortens, akin to bradykinesia (Fig. 2B). We also tested for rescue by neuronal or

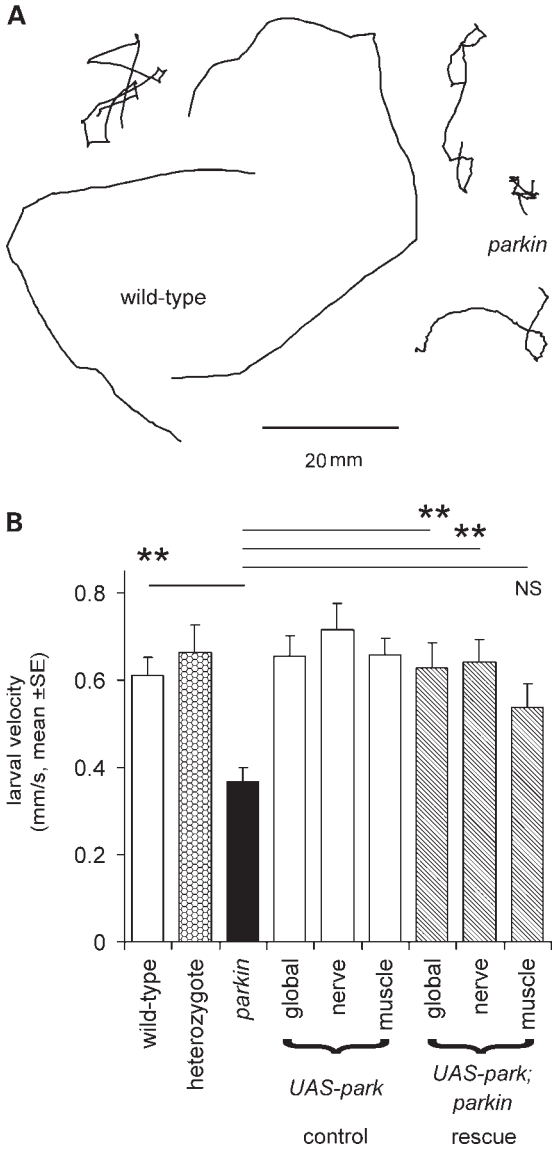

Figure 1. Larval locomotion is reduced in *parkin* mutants. (**A**) Tracks of *parkin* transheterozygotes crawling for 2 min are shorter than those of wild-type. (**B**) Quantification shows that the mean velocity of the *parkin* mutant is 62% of wild-type (Bonferroni *post hoc* comparison: $P = 0.003$). A significant rescue is seen with the expression of wild-type *parkin* in the transheterozygote background using the global or neuronal drivers but not with the muscle driver (Bonferroni *post hoc* tests: $P = 0.009$, 0.003, 0.253, respectively). At least 10 larvae of each genotype, total 130. Genotypes—wild-type: CS/w^-; heterozygote: $CS/park^{z3678}$; *parkin*: $park^{25}/park^{z3678}$. Drivers—global: *Act5C*; neuronal: $elav^{3E1}$; muscle: *G14*. All rescue experiments are in $park^{25}/park^{z3678}$ background.

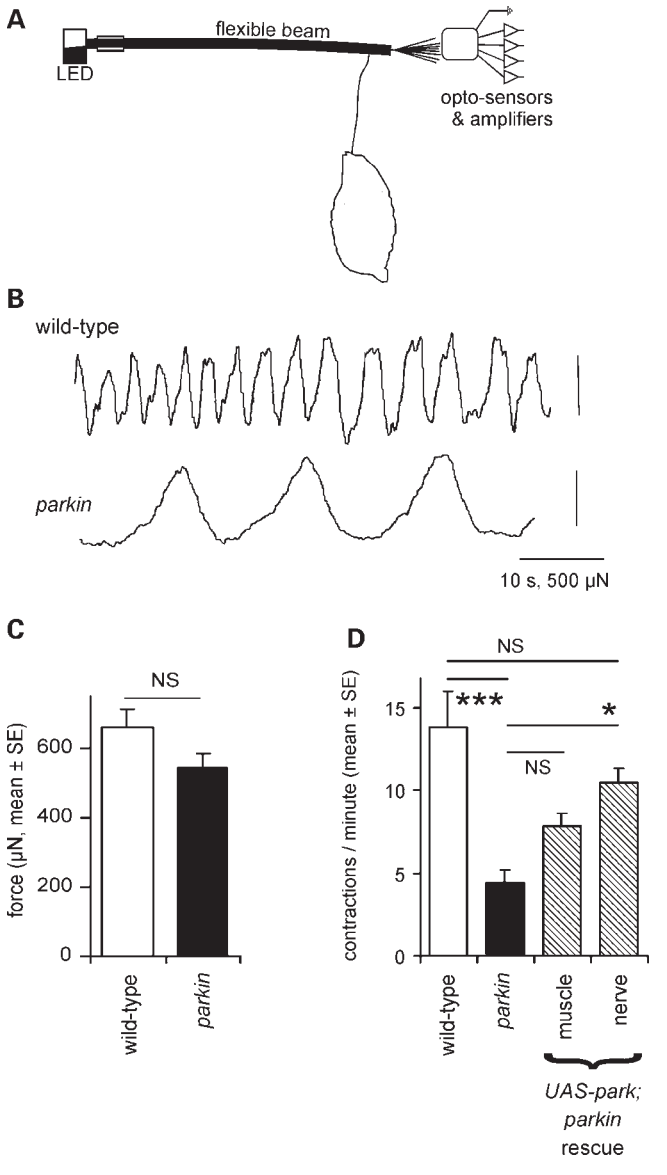

Figure 2. Locomotor contractions are less frequent in *parkin* larvae. (**A**) A larval extensometer, constructed from a flexible photobeam and quadrant photodiode. (**B**) Peristaltic waves recorded by the extensometer show that contractions are fewer in *parkin* knockouts than in wild-type, but the peak–peak excursion is not affected. (**C**) The mean force is the same in wild-type and *parkin* knockout (ANOVA: $F_{1,27} = 2.8$, $P = 0.10$). (**D**) The frequency of peristaltic contractions is reduced in the *parkin* knockout (ANOVA, Bonferroni *post hoc* test, $P < 0.001$), and completely rescued by neuronal expression of wild-type parkin in nerve (Bonferroni *post hoc* test versus *parkin* $P = 0.014$; versus wild-type $P = 0.56$). Expression in muscle is ineffective (Bonferroni $P = 0.38$). Genotypes and number of larvae—wild-type: *CS* 13; *parkin*: $park^{25}/park^{25}$ 15; drivers: neuronal: $elav^{3EI}$ 10; muscle: *G14* 12. Rescues are in $park^{25}/park^{25}$ background.

muscle driver. Only the neuronal driver restored the contraction frequency to wild-type levels (Fig. 2D).

The peristaltic longitudinal muscles are innervated by segmental nerves arising from the ventral nerve cord. To examine the neural input to the muscles, we severed all the segmental nerves and used a suction electrode on a segmental nerve to record the efferent activity of the motoneurons. The wild-type nerve recordings showed regular bursts of action

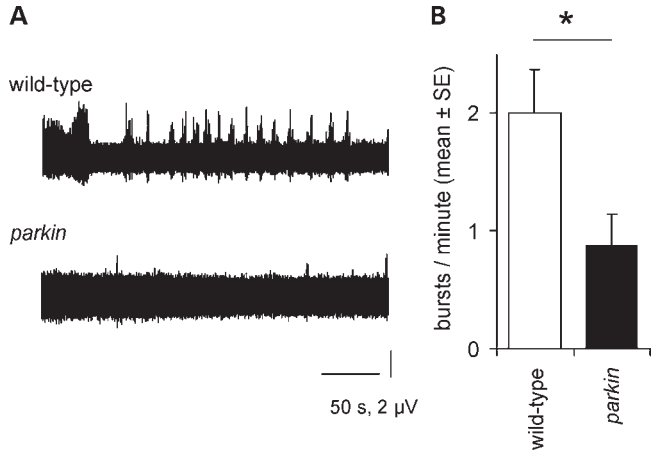

Figure 3. Central pattern generator activity is reduced in *parkin* knockout. (**A**) The frequency of bursts in the motoneurons is reduced in the *parkin* knockout, with the wild-type showing a regular rhythm (and occasional long bursts), while the *parkin* mutant is much quieter. (**B**) The reduction (mean: 56%) is significant (ANOVA $F_{1,9} = 6.1$, $P = 0.039$). Genotypes—wild-type: *CS*; *parkin*: $park^{25}/park^{25}$.

potentials, along with occasional periods of tonic activity (Fig. 3). In the *parkin* null, the frequency of bursts was significantly reduced (to 44% of wild-type; Fig. 3B).

parkin larvae have reduced resting and synaptic membrane potentials

The muscles used in locomotion include the longitudinal body wall muscles 6 and 7. Since their neuromuscular junction is easily accessible, it has been extensively studied, and is now a model synapse (8,18). These muscles are innervated by two motoneurons, so that intracellular recordings from them usually show two sizes of synaptic potentials (19). These are called the Is and Ib excitatory junction potentials (EJPs), though the motoneurons can also be recruited together to produce a composite EJP. Both types of EJPs were present in both the *parkin* muscles (Fig. 4A), but the *parkin* mutant showed significant differences from wild-type.

First, the resting potential of muscles 6/7 was much more positive in the *parkin* larvae than in the controls (Fig. 4A–C): the wild-type resting membrane potential (RMP) is -63.6 ± 1.7 mV (mean $\pm$ SE) and the mean *parkin* -52.9 ± 1.0 mV. We confirmed these data in an independent sample of 292 muscles from two wild-type controls (*CS*, CS/w^{-}) and two *parkin* genotypes ($park^{25}/park^{25}$, $park^{25}/park^{Z3678}$), where the mean difference in RMP was 12.3 mV (nested ANOVA $F_{291,1} = 168$, $P < 0.001$).

Secondly, the size of the EJP was reduced in the *parkin* mutants. The *parkin* knockout might be expected to show smaller synaptic potentials in any case, because the membrane potential of the *parkin* knockout is more positive, and therefore closer to the synaptic reversal potential. However, in recordings made at the same RMP, the *parkin* larvae still had smaller EJPs than the wild-type control. This is shown in Figure 4Ci, where the size of the EJP is plotted as a function of the RMP. The regression line for the wild-type data lies above the regression line for the *parkin* mutants.

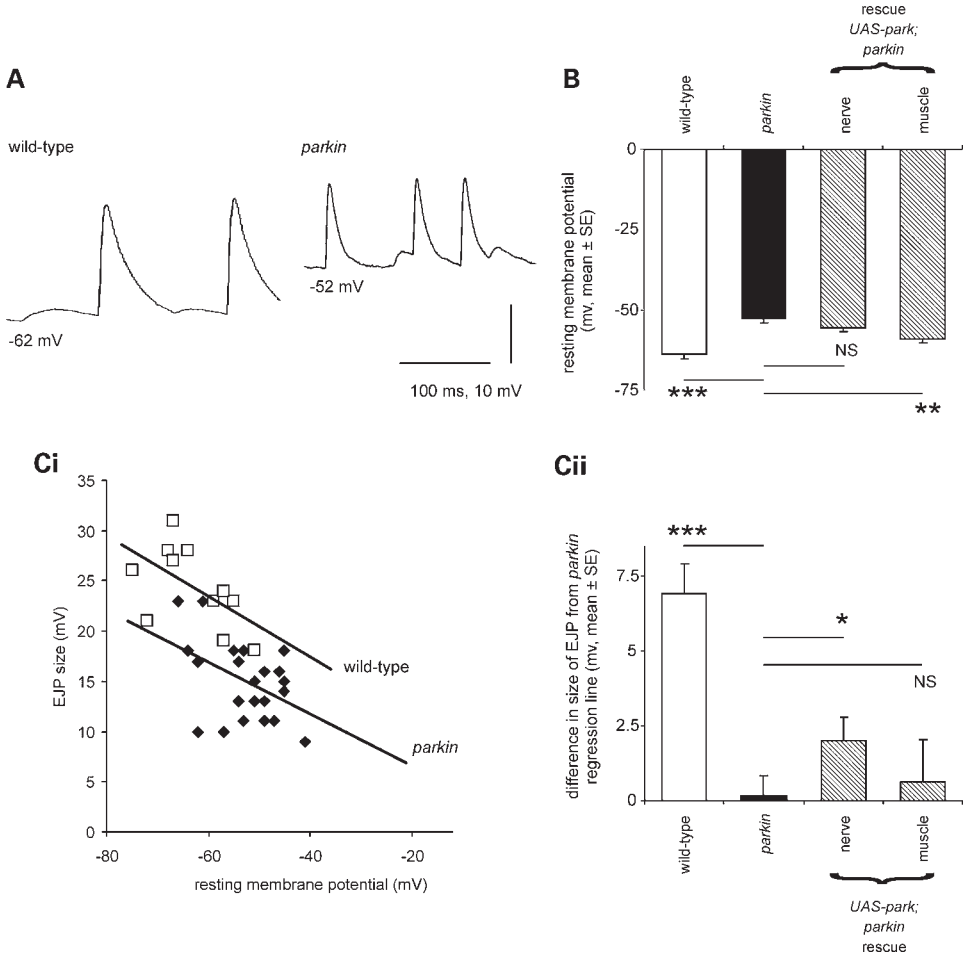

Figure 4. Resting and synaptic potentials are reduced in *parkin* mutants. (**A**) Intracellular recordings from larval muscles show the more positive resting potential in the *parkin* larvae along with smaller EJPs, than in the control, wild-type larva. Both traces show two sizes of spontaneous EJPs: the large ones are called type Is, and the small ones type Ib; additional compound EJPs were also frequently recorded. (**B**) The mean muscle resting membrane potential (RMP) in the *parkin* mutant is 10.7 ± 1.7 mV more positive than the wild-type control (Bonferroni *post hoc* estimate, $P < 0.001$). Expressing wild-type parkin in this transheterozygote background using a neuronal driver did not rescue the RMP deficit (Bonferroni $P = 1.0$), but using a muscle-specific driver a significant rescue was seen (Bonferroni *post hoc* estimate, 6.2 ± 1.5, $P = 0.001$). (**C**) EJPs (type Is) are smaller in *parkin* mutants than in controls. (i) For each genotype, EJPs are smaller at more positive RMPs, but at any given RMP, EJPs from control muscles are bigger than those from *parkin* mutants as indicated by the regression lines. (ii) We tested for rescue as follows: we calculated the *parkin* regression line to provide the expected size of the EJP in each preparation, and calculated the difference of the observed EJP from this expected value. Expressing parkin neuronally in this mutant background partially rescued the EJPs ($t_{13} = 2.6$, $P = 0.023$), but no rescue was seen with muscle expression ($t_{12} = 0.46$, $P = 0.65$). As a control, we checked that the wild-type EJPs are significantly bigger than expected from the *parkin* regression line (one-sample *t*-test: $t_{10} = 6.8$, $P < 0.001$). Data from the same set of muscle recordings as (B); 63 EJPs at least 11 in each genotype. Genotypes—wild-type: CS/w^{-}; *parkin*: $park^{25}/park^{z3678}$. Drivers—neuronal; $elav^{3EI}$; muscle—*G14*. Rescues are all in $park^{25}/park^{z3678}$ background.

We took a sub-sample of our electrophysiological data, using larvae raised on the same batch of food, and tested for rescue of the resting and synaptic potentials by expressing wild-type parkin in nerve or muscle in the transheterozygote background (Fig. 4B, Cii). Muscle expression of *parkin* in the transheterozygote background rescued the muscle RMP by 6.2 ± 1.5 mV (60% of the deficit), but not the synaptic potential, although these data come from the same larvae. On the other hand, the neuronal expression of wild-type *parkin* did not affect the RMP, but did rescue the size of the synaptic potential by 2.0 ± 0.8 mV. (Here we note that the choice of *G14* and $elav^{3E1}$ drivers clearly separated the neuronal and muscle phenotypes.)

The larval neuromuscular junction also shows miniature EJPs (mEJPs): using data from preparations with matched RMPs, the mEJPs from *parkin* transheterozygotes were smaller than those from wild-type larvae (modal amplitude: 0.5 and 0.7 mV, respectively; Fig. 5).

parkin larvae show compromised respiration

The failure to maintain the RMP along with data from adults showing defective mitochondrial fission/fusion (17,20) suggested that the rate at which *parkin* larvae generate ATP by aerobic respiration might be reduced. In order to address this we used two separate technologies—capillary respirometer or an oxygen electrode. The capillary respirometer allows us to follow gas exchange in air, while the oxygen electrode, using larvae immersed in HL3 solution, allows us to examine the impact of respiratory poisons on oxygen

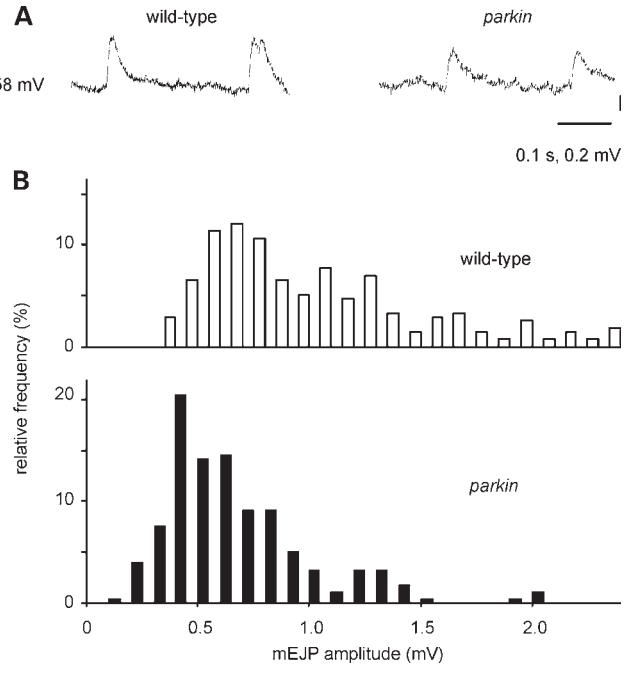

Figure 5. Miniature excitatory junction potentials (mEJPs) are smaller in *parkin* mutants than in wild-type larvae. (**A**) Traces from *parkin* and wild-type larvae. (**B**) Histograms of the amplitude of 550 mEJPs taken from 13 muscles, matched for resting membrane potential (RMP), show that peak amplitude is ~2 mV smaller in the *parkin* larvae (Kolmogorov–Smirnov test statistic 3.5, $P < 0.001$). RMP—wild-type: -63.8 ± 1.1, $n = 7$; *parkin*: -63.0 ± 0.85, $n = 6$. Genotypes—wild-type: CS/w^{-}; parkin: $park^{25}/park^{z3678}$.

consumption. We found with both techniques that the *parkin* larvae had 70% of the oxygen consumption of the wild-type controls (Fig. 6Ai,ii). *parkin* larvae were also more sensitive to metabolic poisons: 6 mM cyanide blocked *parkin* oxygen consumption completely, but reduced only wild-type respiration by 40%, while 6 mM iodoacetate blocked 62% of wild-type respiration, and 87% of *parkin* oxygen consumption (Fig. 6Aii). The ATP levels of the *parkin* knockout larvae were reduced to 14% of the wild-type value (Fig. 6B) and the lactate concentration was nearly doubled (+80%, Fig. 6C). We also obtained similar data in the $park^{25}/park^{Z3678}$ transheterozygotes (mean increase in lactate over wild-type, 88%).

ROS scavengers rescue overgrown synapses, but not membrane potential or locomotor defects in *parkin* larvae

Oxidative stress is frequently associated with PD (in both the human disease and model organisms). Since oxidative stress leads to synaptic overgrowth (16), we counted the synaptic boutons on muscle 6/7 of the third instar *parkin* larvae, as this provides a convenient index of the synapse size. The sample images from the neuromuscular junctions of *parkin* transheterozygotes showed more boutons than those from micrographs of wild-type (*CS*) larvae (Fig. 7A). The average data for boutons/muscle surface area showed that *Drosophila* larvae that are null for *parkin* have ~50% more synaptic boutons than the wild-type controls and heterozygote (Fig. 7B). We confirmed this increase by examining two other wild-type strains (w^{-}, *yw*), a second heterozygote and three other *parkin* mutant combinations: the mean increase was $51 \pm 4\%$ (nested ANOVA $F_{1,371} = 73$, $P < 0.001$). The raw bouton counts from *parkin* mutants were also greater than wild-type (mean increase 18%, nested ANOVA, $F_{1,143} = 37$, $P < 0.001$). To confirm that the increase in boutons is due to the *parkin* knockout, the wild-type parkin was expressed in the *parkin* background, giving a complete rescue of the synaptic overgrowth phenotype (Fig. 7B). Both neuronal and muscle drivers also gave complete rescue of the synaptic overgrowth (Fig. 7B). We confirmed this data in the transheterozygote background, where we find that both neuronal and muscle expression of parkin rescue the synaptic overgrowth (ANOVA, Bonferroni *post hoc* tests, $P < 0.001$, $N = 213$).

Having demonstrated synaptic overgrowth, we wanted to examine the role of oxidative stress in the *parkin* phenotype. Overexpression of genes that scavenge free radicals (*superoxide dismutase*, *catalase*) significantly rescued the overgrowth phenotype, down from 53% to 20% more than the wild-type (Fig. 8A). In contrast to these data, we found no rescue of either the muscle RMP or the larval locomotory defect with expression of any of these scavengers (Fig. 8B and C).

DISCUSSION

We have found that the *parkin* gene knockout and hypomorph have reduced locomotion due to slower movement resembling bradykinesia, reduced synaptic potentials, decreased quantal size, more positive RMP, lower oxygen consumption, reduced ATP and increased lactate, along with overgrown synapses. Our results provide a key description of the interrelated actions of a PD-related gene on the electrophysiology, anatomy and respiration of the most genetically tractable model organism, open to cellular and molecular analysis.

Although several laboratories have generated *parkin* knockouts and hypomorphs (9,17,21,22), only adult phenotypes were reported previously. This is the first report of larval defects associated with mutations in this early-onset gene. Indeed, one group specifically mentioned that they detected no larval phenotype (9). Unlike these groups, we obtain few adult $park^{25}$ or $park^{Z3678}$ homozygotes, so we suspect that the severity of *parkin* phenotypes is affected by differences in food, possibly trace minerals (23,24) that modulate oxidative stress.

Our key observation is that the neuronal *parkin* knockout produces a bradykinesia-like reduction in locomotion. Others have shown loss of mobility in geotaxic assays of adult flies following manipulation of PD-related genes in muscles (11,25). We have taken this further by showing that the larval deficit is neuronal, not muscular as slower peristalsis results from reduced activity in the motoneurons. We show this by two ways: genetically and physiologically. Genetically, we show that (in the early stages of the degeneration) the nervous system is the main tissue affected by *parkin* as we can rescue the locomotory and bradykinesia phenotypes by neuronal expression of wild-type parkin. Physiologically, we show that both synaptic transmission and central pattern

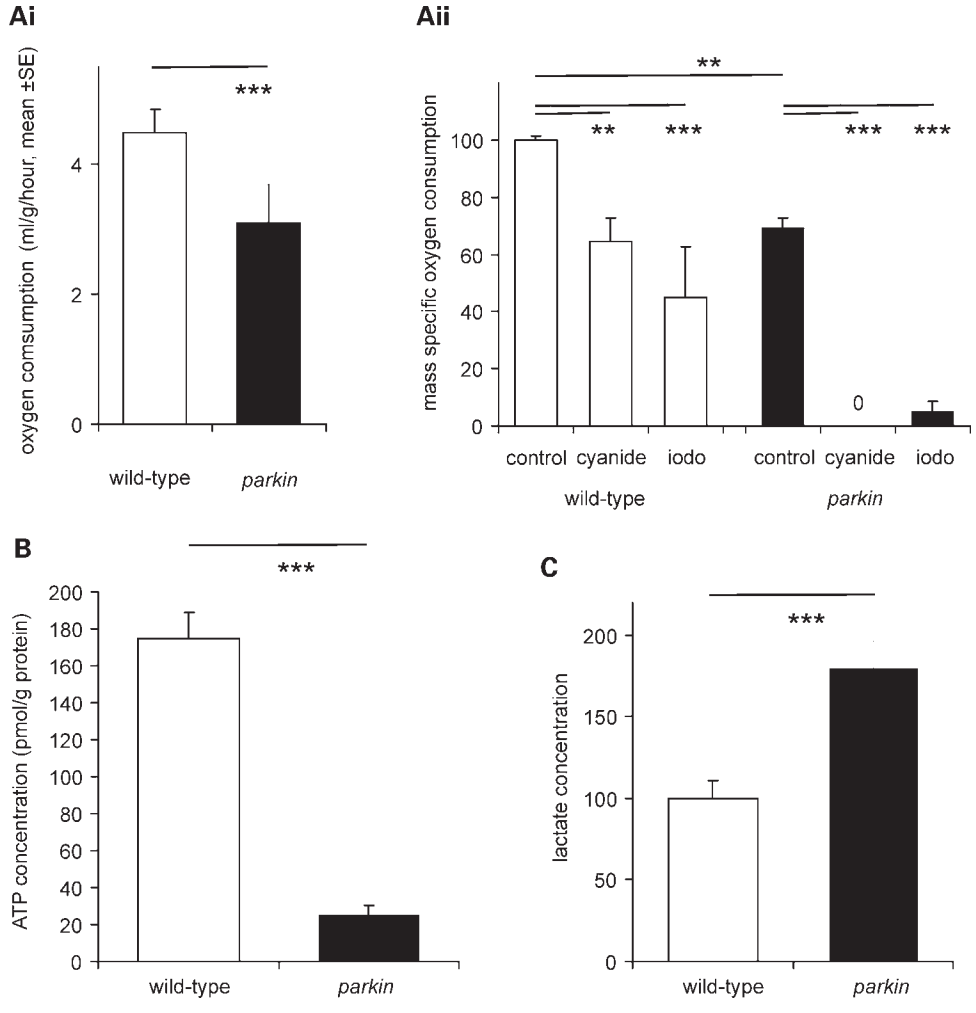

Figure 6. *parkin* larvae have reduced aerobic metabolism and compensate with increased glycolysis. (**A**) Reduction in oxygen consumption. (i) Measurement with a capillary respirometer shows that the oxygen consumption is 70% of the *parkin* larvae than in the wild-type larvae (ANOVA $F_{17,1} = 22.8$, $P < 0.001$). (ii) Measurement with an oxygen electrode confirms that the oxygen consumption of *parkin* is 70% of wild-type (ANOVA $F_{23,1} = 78$, $P < 0.001$). Addition of 6 mM cyanide or iodoacetate reduces respiration, having a bigger impact on the *parkin* than the wild-type larvae. Data normalized to wild-type as 100%. (**B**) The ATP concentration is lower in *parkin* than in the wild-type larvae (ANOVA $F_{15,1} = 104$, $P < 0.001$). (**C**) The lactate concentration is higher in the *parkin* than in the wild-type controls (ANOVA $F_{23,1} = 16$, $P = 0.001$). Data normalized as moles lactate/gram of protein, with wild-type as 100%. Genotypes—wild-type: *CS*; parkin: $park^{25}/park^{25}$.

generator (CPG) activity are reduced. The reduction in CPG activity may result from reduced neurotransmission. The CPG may also be slowed by pumping deficits, as the low levels of ATP will increase the time taken to correct the ionic imbalance that builds up in neurons during each peristaltic wave (26). In addition, locomotion is also modulated by aminergic (dopamine, serotonin etc) neurons that depend on the *Drosophila* vesicular aminergic transporter (DVMAT). Mutations in this gene severely slow crawling (27). Since adult data show an interaction of DVMAT with *parkin* (21), so too, may larval bradykinesia result from *parkin*-induced disruption of aminergic transmission.

The smaller EJPs and mEJPs in the *parkin* knockout indicate a reduction in synaptic transmission. This is most likely to result from reduced glutamate release—perhaps, as a result of problems with its transport into vesicles in an ATP-dependent manner. The recent suggestion that parkin may affect transmission through its interaction with endocytic proteins, e.g. endophilin-A (28) is unlikely to explain our data: although parkin is known to function as a ubiquitin E3 ligase, failure of parkin to ubiquitinate and so degrade endophilin is unlikely to reduce synaptic transmission. A third possibility is that the motoneuron, like the muscle, has a more positive resting potential and this affects the dynamics of glutamate release. Finally, we note that the neuronal rescue did not fully restore the size of the EJP, so that a reduction in muscle impedance or post-synaptic ionic dynamics may also contribute to the reduction in synaptic transmission. Although the original descriptions of the phenotype of *parkin* null mice were divergent (29), more recent evidence indicates that these mice do have reduced dopamine release at striatal synapses (30). At the fly neuromuscular junction, manipulations of another PD-related gene, *LRRK2*, and its *Drosophila* homologue *dLRRK*, show complex effects on synaptic transmission. These include a reduction in synaptic transmitter release in the *dLRRK* knockout (31). However, the other effects of *LRRK2*

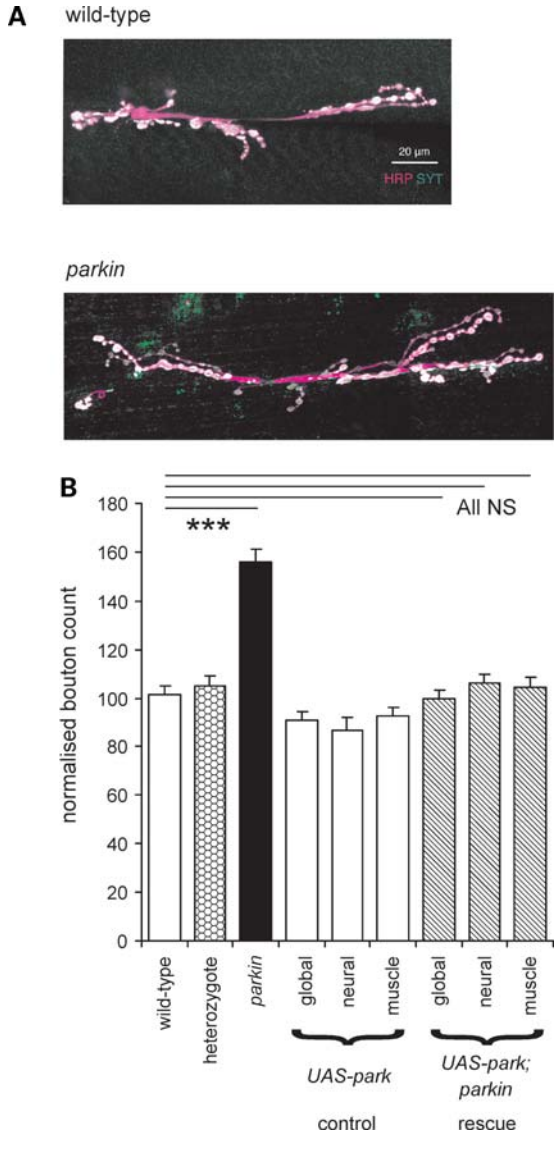

Figure 7. Overgrown synapses are characteristic of *parkin* mutants. (**A**) There are more boutons (white) in the *parkin* neuromuscular junction than in the control wild-type. Images from confocal stacks of synaptic terminals on muscles 6 and 7 stained with horseradish peroxidase antibody (HRP, magenta) show the neuronal membrane and with synaptotagmin (SYT, green) antibody to show the terminal boutons. (**B**) Quantification of the bouton count at 372 synapses confirms that *parkin* mutants have excess boutons (+53%, Bonferroni $P < 0.001$). Expression of wild-type *parkin* by the global, neuronal or muscle drivers achieves substantial rescue of the synaptic overgrowth (down to 3% above the control values, Bonferroni comparison with wild-type each = 1.0). There is no significant difference between the synaptic overgrowth in the three rescues (ANOVA, $F_{2,78} = 0.81$, $P < 0.445$). At least 16 neuromuscular junctions for each genotype, totally 223. Data normalized as ratio of boutons/muscle area, with wild-type as 100%. Genotypes—wild-type: *CS*; *parkin*: $park^{25}/park^{25}$. Drivers—global: *Act5C;* neuronal; $elav^{3EI}$; muscle: *G14*. Rescues are in $park^{25}/park^{25}$ background.

and *parkin* manipulations are dissimilar, indicating that these genes may not always be acting through a common cellular mechanism.

The more positive RMP in our *parkin* larvae is most likely to be due to a reduction in ATP synthesis, which requires oxygen. We have demonstrated this using two techniques to record O_2 consumption and by measuring ATP levels directly. A similar reduction in ATP production (by 58%) is reported in human fibroblasts from patients with *parkin* mutations (32). Low ATP will lead to reduced pumping of ions across the membrane and so a more positive RMP (although this may be counteracted by increased opening of ATP-sensitive potassium channels (33)). Reports of *Drosophila* mutants with a more positive membrane potential are rare, but in one, the phosphoglycerate kinase mutant, *nubian*, this is due to reduced ATP levels (34). In the *parkin* knockout, we predict that neurons (as well as muscles) will also have a more positive membrane potential because the mutation is expressed globally.

The reduction of oxygen consumption indicates severe mitochondrial dysfunction; not surprising in the light of the reports of deficient mitochondrial fission/fusion and mitochondrial swelling in a range of fly models of PD (3,17,20,35). The *parkin* larvae respond to this by increasing glycolysis, as indicated by the increase in lactate levels. Increased lactate has been reported in some PD patients (36), but not in others (37). This discrepancy might be due to a general increase in lactate (and changes in anaerobic metabolism) with age (38), and so our data, along with improvements in genotyping and other molecular techniques may make the role of glycolytic biomarkers in the progression of PD worth revisiting.

Mitochondrial dysfunction will also induce oxidative stress. A key response to oxidative stress is the induction of autophagy (15), which causes increased growth of neuronal terminals (16). As with our *parkin*, so also manipulations of a second PD-related gene, *dLRRK* cause overgrowth of the larval neuromuscular junction (31). We note that, in both transgenics, the overgrowth phenotype is effectively rescued by global, neuronal or muscle expression of wild-type protein. This shows a difference from our physiological and locomotor phenotypes, which were rescued by neuronal—but not muscle—expression of parkin.

We find excellent rescue of the neuronal overgrowth by relieving oxidative stress. Increased expression of cytosolic (*catalase*, *superoxide dismutase* 1) or mitochondrial (*superoxide dismutase* 2) enzymes that scavenge ROS are equally effective. Similarly, adult fly models of PD are rescued by overexpression of genes that reduce ROS, e.g. glutathione *S*-transferase or thioredoxin (11–14).

However, over-expressing oxidative stress transgenes rescues only the neuronal overgrowth; the RMP and locomotor phenotype are not affected. (This is a major contrast to parkin expression, which rescues each of the oxidative stress, RMP and locomotor phenotypes.) Thus, expression of the ROS scavengers exposes fundamental physiological deficits, including the failure to maintain the RMP and the failure of the neuronal network of the CPG. In the same way, antioxidants like vitamin E have powerful cellular actions, but are not generally effective in the treatment of PD patients (39,40).

In conclusion, we find that *parkin* mutants recapitulate the bradykinesia symptoms of PD, and we suggest that this is due to an energy deficit rather than oxidative stress. *parkin*-Dependent mitochondrial dysfunction reduces ATP levels and the ability of neurons to maintain an RMP. Oxidative stress has received considerable attention as a target for treating ageing and neurodegenerative disorders; however, this

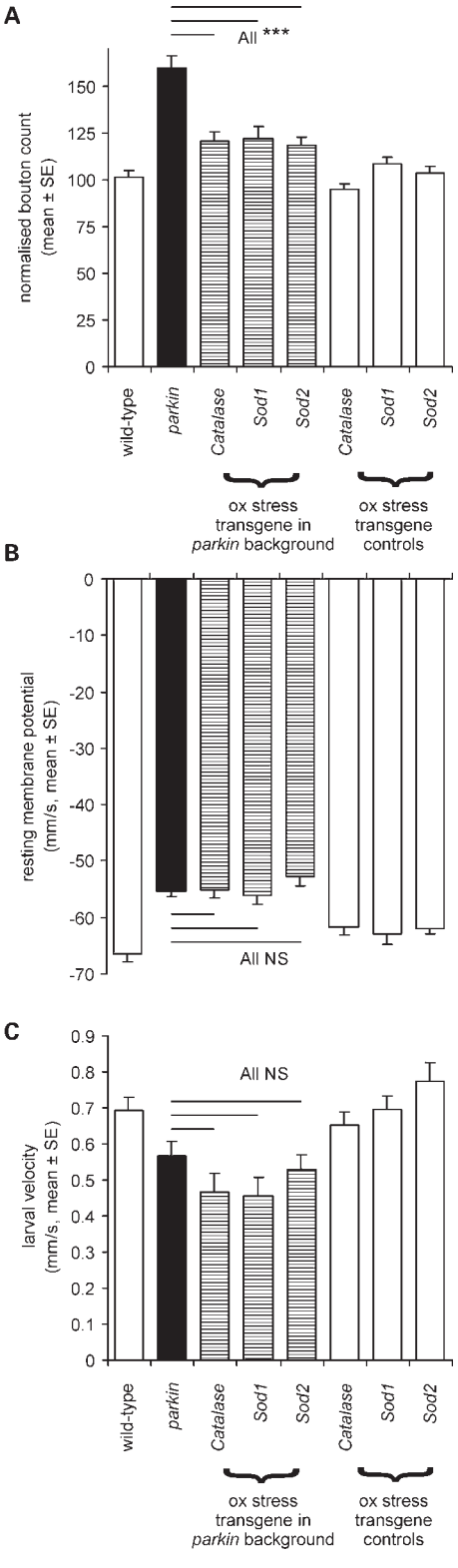

Figure 8. In the *parkin* null background, overexpression of oxidative stress transgenes rescues synaptic overgrowth but not muscle RMP or larval locomotion. (**A**) The normalized bouton count is reduced from the *parkin* mutant peak (~+50% of the CS wild-type) to +20% by overexpression of *catalase* or *superoxide dismutase* (*Sod1* or *Sod2*) with a global driver. The effect of the oxidative stress transgenes is significant (Bonferroni comparison with *parkin* $P < 0.001$ for each transgene). At least 24 neuromuscular junctions for each genotype, totally 224. (**B**) Oxidative stress gene overexpression did not rescue the muscle RMP (comparison with *parkin* mutants, Bonferroni tests all $P = 1.0$). At least 18 muscles for each genotype, 213 in total. (**C**) The oxidative stress gene overexpression did not rescue larval locomotion (comparison with *parkin* mutants Bonferroni tests all $P = 1.0$). At least 12 larvae for each genotype, total 171. Genotypes—(A and C) wild-type: *CS*; *parkin*: $park^{25}/park^{25}$ outcrossed to the *Act5C* driver used to express each transgene in $park^{25}/park^{25}$ background. (B) Wild-type CS/w^{-}; *parkin*; $park^{Z3678}/park^{25}$, transgene expression driven by the *Act5C* driver.

study suggests that energy metabolism is a more important target for the treatment of PD.

MATERIALS AND METHODS

Flies

Flies were routinely raised at 25°C. Wild-type flies (*Canton-S*, CS and w^{-}, w^{1118}) were obtained from our laboratory stocks, while the $parkin^{25}$ (17), $parkin^{Z3678}$ (11) and UAS-$parkin^{C2}$ (wild-type *Drosophila parkin* (11)) lines were a gift from Alex Whitworth & Leo Pallanck. The *G14* GAL4 line (from Akinao Nose, Tokyo), UAS stocks and *Actin5C* and $elav^{3E1}$ GAL4 lines (from the Bloomington Stock centre) were recombined with the *parkin* lines as required. All experiments were performed on the third instar larvae, selected as they crawled on the side of the vial or over the surface of the food.

In all experiments, we find significant differences between the *Canton-S* (CS) wild-type and $park^{25}/park^{25}$ null. When we compare the wild-type outcross, CS/w^{-} and the $park^{25}/park^{Z3678}$ transheterozygote, we observe the same effects. All the parkin rescue experiments were performed both in the null background and the transheterozygote background; we find no differences due to background.

Larval locomotion

Larval locomotion was recorded using our standard procedure (41). Larval progress across a horizontal agar-filled Petri dish was recorded on to a computer disk for 2 min at a frame rate of 12 frames/min. Positions were determined using the MTrack2 plugin (42) (see also online http://valelab.ucsf.edu/~nico/IJplugins/MTrack2.html) to ImageJ (http://rsbweb.nih.gov/ij/).

Larval length assay

Larval length assay was performed as described recently (41). A larva pulls on a flexible plastic optical pipe, through which the beam of a red LED is transmitted onto a photodetector. The four optosensors in the detector allow the linear movement of the beam to be computed, with the signal recorded on computer disk at 0.1 Hz.

Saline solution

All experiments were performed in HL3 solution (43). Composition in millimolars—sodium chloride, 70; potassium chloride, 5; calcium chloride, 1; sodium hydrogen carbonate, 10; BES (*N*,*N*-bis(2-hydroxyethyl)-2-aminoethanesulphonic acid), 5; trehalose, 5; sucrose, 115; pH 7.5.

Segmental nerve recordings

Segmental nerve recordings were made by dissecting open the larva in HL3 saline, and removing its gut, fat body and reproductive organs. The segmental nerves were all severed and the CNS end of one drawn up into a glass suction pipette. The signal was amplified 1000 times and recorded on disk at 10 kHz.

Intracellular recording from the longitudinal muscles

Intracellular recording from the longitudinal muscles 6/7 was made with sharp glass micropipettes, with tip resistance 10–15 MΩ. A high-resistance input 50× amplifier was used, and data stored on computer disk at 5 kHz. All data were recorded in HL3 saline. Spontaneous EJPs were recorded from preparations in which the CNS was left in place with intact innervation and the size of the large (Is) EJPs measured; mEJPs were analysed in preparations from which the CNS had been removed. Data from larvae with the RMP more positive than −40 mV were discarded.

Oxygen consumption

Oxygen consumption was recorded with two techniques. Firstly, using a capillary respirometer three larvae were placed in an unfilamented borosilicate glass capillary (internal diameter 1.16 mm, length 150 mm; Clark Electromedical, Pangbourne, UK) and one end sealed with cotton wool/nail varnish. Carbon dioxide was absorbed by ∼2 mg sodium hydroxide, and the volume change monitored by the movement of a paraffin oil droplet. The respiratory quotient was determined from larvae tested with and without the hydroxide to absorb carbon dioxide. No movement of the paraffin droplet was seen in replicates without larvae. Experiments were all performed at 21°C. Secondly, using a Clark oxygen electrode, in which larvae to a mass of 50 mg (∼30–40 larvae) were placed in the recording chamber filled with 3 ml HL3 saline.

ATP and lactate were measured in larval haemolymph using kits from proteinkinase.de (Kassel, Germany) and Eton Biosciences Inc. (San Diego, USA), respectively, following the manufacturers' protocols. Bradford assays (44) were used to measure the protein concentrations in the samples.

Synaptic boutons

Synaptic boutons were counted as described previously (16), using a polyclonal synaptotagmin antibody to mark synaptic-release sites and horseradish peroxidase antiserum to mark the nerve membrane.

Statistics

Statistics were evaluated in SPSS. In experiments with multiple genotypes, ANOVA followed by *post hoc* tests were used to compare two genotypes and nested ANOVA to compare groups of related genotypes (e.g. all *parkin* lines with all wild-type lines). Where Bonferroni probabilities are reported, at least the same probability level was seen in the Tukey HSD test. In the figures, NS denotes not significant and $^{*}P < 0.05$, $^{**}P < 0.01$, $^{***}P < 0.001$.

ACKNOWLEDGEMENTS

We thank Alex Whitworth (University of Sheffield) for fly stocks, Harry Whitwell for assistance with experiments.

Conflict of Interest statement: None declared.

FUNDING

This work was supported by the Parkinson's Disease Society (now Parkinson's UK, Grant K-0804), BBSRC (for studentship to A.V.), The UK Medical Research Council project grant G0400580 (S.T.S.) and The Wellcome Trust, and Nuffield Foundation for funding. We are grateful to John Sparrow and Sangeeta Chawla for their comments on the manuscript. Funding to pay the Open Access publication charges for this article was provided by the Wellcome Trust.

REFERENCES

1. Hardy, J. (2010) Genetic analysis of pathways to Parkinson disease. *Neuron*, **68**, 201–206.
2. Dawson, T.M., Ko, H.S. and Dawson, V.L. (2010) Genetic animal models of Parkinson's disease. *Neuron*, **66**, 646–661.
3. Whitworth, A.J. (2011) *Drosophila* models of Parkinson's disease. *Adv. Genet.*, **73**, 1–50.
4. Lu, B. (2009) Recent advances in using *Drosophila* to model neurodegenerative diseases. *Apoptosis*, **14**, 1008–1020.
5. Botella, J.A., Bayersdorfer, F., Gmeiner, F. and Schneuwly, S. (2009) Modelling Parkinson's disease in *Drosophila*. *NeuroMol. Med.*, **11**, 268–280.
6. Venken, K., Simpson, J. and Bellen, H. (2011) Genetic manipulation of genes and cells in the nervous system of the fruit fly. *Neuron*, **72**, 202–230.
7. Tain, L.S., Mortiboys, H., Tao, R.N., Ziviani, E., Bandmann, O. and Whitworth, A.J. (2009) Rapamycin activation of 4E-BP prevents Parkinsonian dopaminergic neuron loss. *Nat. Neurosci.*, **12**, 1129–1135.
8. Budnik, V. and Ruiz-Canada, C. (2006) *The fly neuromuscular junction: structure and function*, 2nd edn. Academic Press, San Diego, CA, USA.
9. Pesah, Y., Pham, T., Burgess, H., Middlebrooks, B., Verstreken, P., Zhou, Y., Harding, M., Bellen, H. and Mardon, G. (2004) *Drosophila* parkin mutants have decreased mass and cell size and increased sensitivity to oxygen radical stress. *Development*, **131**, 2183–2194.
10. Meulener, M., Whitworth, A.J., Armstrong-Gold, C.E., Rizzu, P., Heutink, P., Wes, P.D., Pallanck, L.J. and Bonini, N.M. (2005) *Drosophila* DJ-1 mutants are selectively sensitive to environmental toxins associated with Parkinson's disease. *Curr. Biol.*, **15**, 1572–1577.
11. Whitworth, A.J., Theodore, D.A., Greene, J.C., Benes, H., Wes, P.D. and Pallanck, L.J. (2005) Increased glutathione S-transferase activity rescues dopaminergic neuron loss in a *Drosophila* model of Parkinson's disease. *Proc. Natl Acad. Sci. USA*, **102**, 8024–8029.
12. Im, J.Y., Lee, K.W., Junn, E. and Mouradian, M.M. (2010) DJ-1 protects against oxidative damage by regulating the thioredoxin/ASK1 complex. *Neurosci. Res.*, **67**, 203–208.
13. Umeda-Kameyama, Y., Tsuda, M., Ohkura, C., Matsuo, T., Namba, Y., Ohuchi, Y. and Aigaki, T. (2007) Thioredoxin suppresses Parkin-associated endothelin receptor-like receptor-induced neurotoxicity and extends longevity in *Drosophila*. *J. Biol. Chem.*, **282**, 11180–11187.
14. Botella, J.A., Bayersdorfer, F. and Schneuwly, S. (2008) Superoxide dismutase overexpression protects dopaminergic neurons in a *Drosophila* model of Parkinson's disease. *Neurobiol. Dis.*, **30**, 65–73.
15. Shen, W. and Ganetzky, B. (2009) Autophagy promotes synapse development in *Drosophila*. *J. Cell. Biol.*, **187**, 71–79.

16. Milton, V.J., Jarrett, H.E., Gowers, K., Chalak, S., Briggs, L., Robinson, I.M. and Sweeney, S.T. (2011) Oxidative stress induces overgrowth of the *Drosophila* neuromuscular junction. *Proc. Natl Acad. Sci. USA*, **108**, 17521–17526.
17. Greene, J.C., Whitworth, A.J., Kuo, I., Andrews, L.A., Feany, M.B. and Pallanck, L.J. (2003) Mitochondrial pathology and apoptotic muscle degeneration in *Drosophila* parkin mutants. *Proc. Natl Acad. Sci. USA*, **100**, 4078–4083.
18. Bellen, H.J., Tong, C. and Tsuda, H. (2010) 100 years of *Drosophila* research and its impact on vertebrate neuroscience: a history lesson for the future. *Nat. Rev. Neurosci.*, **11**, 514–522.
19. Kurdyak, P., Atwood, H.L., Stewart, B.A. and Wu, C.F. (1994) Differential physiology and morphology of motor axons to ventral longitudinal muscles in larval *Drosophila*. *J. Comp. Neurol.*, **350**, z463–472.
20. Poole, A.C., Thomas, R.E., Andrews, L.A., McBride, H.M., Whitworth, A.J. and Pallanck, L.J. (2008) The PINK1/Parkin pathway regulates mitochondrial morphology. *Proc. Natl Acad. Sci. USA*, **105**, 1638–1643.
21. Sang, T.K., Chang, H.Y., Lawless, G.M., Ratnaparkhi, A., Mee, L., Ackerson, L.C., Maidment, N.T., Krantz, D.E. and Jackson, G.R. (2007) A *Drosophila* model of mutant human Parkin-induced toxicity demonstrates selective loss of dopaminergic neurons and dependence on cellular dopamine. *J. Neurosci.*, **27**, 981–992.
22. Cha, G.H., Kim, S., Park, J., Lee, E., Kim, M., Lee, S.B., Kim, J.M., Chung, J. and Cho, K.S. (2005) Parkin negatively regulates JNK pathway in the dopaminergic neurons of *Drosophila*. *Proc. Natl Acad. Sci. USA*, **102**, 10345–10350.
23. Saini, N. and Schaffner, W. (2010) Zinc supplement greatly improves the condition of parkin mutant *Drosophila*. *Biol. Chem.*, **391**, 513–518.
24. Saini, N., Oelhafen, S., Hua, H., Georgiev, O., Schaffner, W. and Bueler, H. (2010) Extended lifespan of *Drosophila* parkin mutants through sequestration of redox-active metals enhancement of anti-oxidative pathways. *Neurobiol. Dis.*, **40**, 82–92.
25. Feany, M.B. and Bender, W.W. (2000) A *Drosophila* model of Parkinson's disease. *Nature*, **404**, 394–398.
26. Pulver, S.R. and Griffith, L.C. (2010) Spike integration and cellular memory in a rhythmic network from Na+/K+ pump current dynamics. *Nat. Neurosci.*, **13**, 53–59.
27. Simon, A.F., Daniels, R., Romero-Calderon, R., Grygoruk, A., Chang, H.Y., Najibi, R., Shamouelian, D., Salazar, E.D., Solomon, M., Ackerson, L.C. *et al.* (2009) *Drosophila* vesicular monoamine transporter mutants can adapt to reduced or eliminated vesicular stores of dopamine and serotonin. *Genetics*, **181**, 525–541.
28. Trempe, J.F., Chen, C.X.Q., Grenier, K., Camacho, E.M., Kozlov, G., McPherson, P.S., Gehring, K. and Fon, E.A. (2009) SH3 domains from a subset of BAR proteins define a Ubl-binding domain and implicate Parkin in synaptic ubiquitination. *Mol. Cell.*, **36**, 1034–1047.
29. Perez, F.A. and Palmiter, R.D. (2005) Parkin-deficient mice are not a robust model of parkinsonism. *Proc. Natl Acad. Sci. USA*, **102**, 2174.
30. Kitada, T., Pisani, A., Karouani, M., Haburcak, M., Martella, G., Tscherter, A., Platania, P., Wu, B., Pothos, E.N. and Shen, J. (2009) Impaired dopamine release and synaptic plasticity in the striatum of Parkin−/− mice. *J. Neurochem.*, **110**, 613–621.
31. Lee, S., Liu, H.P., Lin, W.Y., Guo, H. and Lu, B. (2010) LRRK2 kinase regulates synaptic morphology through distinct substrates at the presynaptic and postsynaptic compartments of the *Drosophila* neuromuscular junction. *J. Neurosci.*, **30**, 16959–16969.
32. Mortiboys, H., Thomas, K.J., Koopman, W.J.H., Klaffke, S., bou-Sleiman, P., Olpin, S., Wood, N.W., Willems, P.H.G.M., Smeitink, J.A.M. and Cookson, M.R. (2008) Mitochondrial function and morphology are impaired in parkin-mutant fibroblasts. *Ann. Neurol.*, **64**, 555–565.
33. Liss, B., Haeckel, O., Wildmann, J., Miki, T., Seino, S. and Roeper, J. (2005) K-ATP channels promote the differential degeneration of dopaminergic midbrain neurons. *Nat. Neurosci.*, **8**, 1742–1751.
34. Wang, P., Saraswati, S., Guan, Z., Watkins, C.J., Wurtman, R.J. and Littleton, J.T. (2004) A *Drosophila* temperature-sensitive seizure mutant in phosphoglycerate kinase disrupts ATP generation and alters synaptic function. *J. Neurosci.*, **24**, 4518.
35. Ziviani, E., Tao, R.N. and Whitworth, A.J. (2010) *Drosophila* Parkin requires PINK1 for mitochondrial translocation and ubiquitinates Mitofusin. *Proc. Natl Acad. Sci. USA*, **107**, 5018.
36. Bowen, B.C., Block, R.E., Sanchez-Ramos, J., Pattany, P.M., Lampman, D.A., Murdoch, J.B. and Quencer, R.M. (1995) Proton MR spectroscopy of the brain in 14 patients with Parkinson disease. *Am. J. Neuroradiol.*, **16**, 61–68.
37. Yamamoto, M., Ujike, H., Wada, K. and Tsuji, T. (1997) Cerebrospinal fluid lactate and pyruvate concentrations in patients with Parkinson's disease and mitochondrial encephalomyopathy, lactic acidosis, and stroke-like episodes (MELAS). *J. Neurol. Neurosurg. Psych.*, **62**, 290.
38. Ross, J.M., Oberg, J., Brene, S., Coppotelli, G., Terzioglu, M., Pernold, K., Goiny, M., Sitnikov, R., Kehr, J., Trifunovic, A. *et al.* (2010) High brain lactate is a hallmark of aging and caused by a shift in the lactate dehydrogenase A/B ratio. *Proc. Natl Acad. Sci. USA*, **107**, 20087–20092.
39. Parkinson Study Group. (1993) Effects of tocopherol and deprenyl on the progression of disability in early Parkinson's disease. N. Engl. J. Med., **328**, 176–183.
40. Löhle, M. and Reichmann, H. (2010) Clinical neuroprotection in Parkinson's disease: still waiting for the breakthrough. *J. Neurol. Sci.*, **289**, 104–114.
41. Hill, J.A. (2008) The roles of tyramine and octopamine in *Drosophila melanogaster*. PhD Thesis, University of York.
42. Klopfenstein, D.R. and Vale, R.D. (2004) The lipid binding pleckstrin homology domain in UNC-104 kinesin is necessary for synaptic vesicle transport in *Caenorhabditis elegans*. *Mol. Biol. Cell.*, **15**, 3729–3739.
43. Stewart, B.A., Atwood, H.L., Renger, J.J., Wang, J. and Wu, C.F. (1994) Improved stability of *Drosophila* larval neuromuscular preparations in haemolymph-like physiological solutions. *J. Comp. physiol. A*, **175**, 179–191.
44. Bradford, M.M. (1976) A rapid and sensitive method for the quantitation of microgram quantities of protein utilizing the principle of protein-dye binding. *Anal. Biochem.*, **72**, 248–254.